Available online at www.sciencedirect.com

SciVerse ScienceDirect

Journal of Nutritional Biochemistry 23 (2012) 140–152

Journal of Nutritional Biochemistry

Postnatal growth velocity modulates alterations of proteins involved in metabolism and neuronal plasticity in neonatal hypothalamus in rats born with intrauterine growth restriction☆

Marie-Cécile F. Alexandre-Gouabau[a,*], Emilie Bailly[a], Thomas L. Moyon[a], Isabelle C. Grit[a], Bérengère Coupé[a], Gwenola Le Drean[a], Hélène J. Rogniaux[b], Patricia Parnet[a]

[a]INRA and University of Nantes, UMR-1280 Physiologie des Adaptations Nutritionnelles CHU Hôtel Dieu, 44093 Nantes cedex 1, France
[b]INRA UR1268 Biopolymères Interactions Assemblages, Plate-Forme BIBS, F-44300 Nantes, France

Received 9 July 2010; received in revised form 9 November 2010; accepted 9 November 2010

Abstract

Intrauterine growth restriction (IUGR) due to maternal protein restriction is associated in rats with an alteration in hypothalamic centers involved in feeding behaviour. In order to gain insight into the mechanism of perinatal maternal undernutrition in the brain, we used proteomics approach to identify hypothalamic proteins that are altered in their expression following protein restriction *in utero*. We used an animal model in which restriction of the protein intake of pregnant rats (8% vs. 20%) produces IUGR pups which were randomized to a nursing regimen leading to either rapid or slow catch-up growth. We identified several proteins which allowed, by multivariate analysis, a very good discrimination of the three groups according to their perinatal nutrition. These proteins were related to energy-sensing pathways (Eno 1, E_2PDH, Acot 1 and Fabp5), redox status (Bcs 1L, PrdX3 and 14-3-3 protein) or amino acid pathway (Acy1) as well as neurodevelopment (DRPs, MAP2, Snca). In addition, the differential expressions of several key proteins suggested possible shunts towards ketone-body metabolism and lipid oxidation, providing the energy and carbon skeletons necessary to lipogenesis. Our results show that maternal protein deprivation during pregnancy only (IUGR with rapid catch-up growth) or pregnancy and lactation (IUGR with slow postnatal growth) modulates numerous metabolic pathways resulting in alterations of hypothalamic energy supply. As several of these pathways are involved in signalling, it remains to be determined whether hypothalamic proteome adaptation of IUGR rats in response to different postnatal growth rates could also interfere with cerebral plasticity or neuronal maturation.

Keywords: Intrauterine growth restriction; Hypothalamus; Proteomics; Metabolism

1. Introduction

It is becoming increasingly apparent that nutritional or environmental stimuli, acting during development both *in utero* and during critical periods of relative plasticity beyond birth, may have a lasting impact on cellular structure and function and, consequently, on the risk of developing chronic disease in adulthood [1]. Low birth weight, defined as a birth weight below the 10th percentile for gestational age, is a consequence of intrauterine growth retardation (IUGR) and affects up to 10% of neonates. Intrauterine growth retardation can arise from uteroplacental insufficiency, inadequacies in maternal diet or infection. Infants born with a low birth weight are exposed to a higher risk of developing obesity, type 2 diabetes, coronary heart disease and hypertension in adulthood [2] and also to a large array of cognitive disorders [3]. Infants with IUGR are indeed exposed, not only to *in utero* nutrient deprivation, but to the effects of early postnatal nutrition as well, which can determine postnatal growth rate and has striking consequences on the relative risk of becoming obese. Infants who suffer IUGR but experience rapid postnatal catch-up growth by 2 years of age are fatter infants [4] and have a greater

Abbreviations: IUGR, intrauterine growth retardation; PND, postnatal day; CC, control; RC, IUGR with rapid postnatal catch-up growth; RR, IUGR with slow postnatal growth; 2-DE, two-dimensional gel electrophoresis; IPG, immobilized pH gradient; SDS, sodium dodecyl sulphate; PAGE, polyacrylamide gel electrophoresis; MS, mass spectrometry; LC-MS/MS, liquid chromatography-tandem mass spectrometry; PCA, principal component analysis; PLS-DA, partial least-squares discriminant analysis; GO, Gene Ontology.

☆ Supported by a grant from the Agence Nationale de la Recherche (ANR PNRA Grant 2005-2009). B.C. was sponsored by a doctoral fellowship from Institut National de la Recherche Agronomique and Région Pays de la Loire and granted by La Fondation Louis Bonduelle (France).

* Corresponding author at: Institut National de la Recherche Agronomique, Unité Mixte de Recherche 1280, Laboratoire de Physiologie des Adaptations Nutritionnelles, Centre Hospitalier Universitaire Hôtel-Dieu, Place Alexis Ricordeau, HNB1, 44093 Nantes Cedex 1, France. Tel.: +33 2 53 48 20 12; fax: +33 2 53 48 20 03.

E-mail address: marie-cecile.alexandre-gouabau@univ-nantes.fr (M.-C.F. Alexandre-Gouabau).

0955-2863/$ - see front matter © 2012 Elsevier Inc. All rights reserved.
doi:10.1016/j.jnutbio.2010.11.008

risk of becoming obese in adulthood [5,6]. The fact that nutrition in early life (during both the fetal and neonatal periods) may impact on the later risk of disease led to the concept of metabolic programming or nutritional imprinting [2]. Yet, the underlying molecular mechanisms remain poorly understood. Metabolic programming is demonstrated in experimental models of IUGR produced either by ligation of uterine arteries or by maternal undernutrition during gestation, followed either by rapid catch-up growth or by slow postnatal growth [7]. In a model of impaired early growth due to maternal protein restriction in rats [1], an asymmetric alteration in tissue growth is reported, leading to a preservation of brain growth at the expense of other organs such as the pancreas and kidney. This suggests that fetal malnutrition may induce physiological and/or metabolic adaptations so as to ensure nutrient supply to the most vital organs in order to enhance the chances of fetal survival [2]. In addition, exposure of rats to low-protein diets in both the fetal and suckling periods alters the volume of key hypothalamic centers and changes the neuronal density [8], leading to alterations in the brain response to anorexigenic and orexigenic peptides [6] which may impact on feeding behaviour [9].

We hypothesized that (a) protein restriction *in utero* leads to alterations in the energy balance of the brain and its plasticity and (b) the pattern of growth (either rapid catch-up growth or slow postnatal growth) in the first weeks of postnatal life further modulates these brain alterations. For this purpose, we used an animal model in which restriction of the protein intake of pregnant rats (8% vs. 20%) produces IUGR pups. The offsprings were then randomized to a nursing regimen leading either to rapid catch-up growth or to slow postnatal growth to investigate the effects of perinatal maternal undernutrition on the brain. The profile of expression of hypothalamic proteins of the IUGR pups was assessed compared to control pups using proteomics technology in order to gain insight into modulated developmental events by identifying key proteins potentially involved in the short-term consequences of a low birth weight. Up to now, proteomics has been used to identify and quantify the effect of aging or stress on human, rat and mouse brain proteins [10–12] or to reveal alterations in neurological disorders such as Alzheimer [13,14] or Parkinson's [15] diseases. To our knowledge, in the nutrition field, only one proteomic study has identified the specific proteins modulated by a dietary supplement (polyphenols) in the rat brain in the absence of disease [16]. The effects of perinatal undernutrition on brain proteome have not yet been addressed.

In the current study, we chose to examine the hypothalamus as the target of IUGR because it plays a key regulatory role in homeostasis. Hypothalamus receives and integrates a wide array of information and acts as a sensor for extracellular nutrients, humoral and neuronal signals necessary to regulate a multitude of body functions such as tissue metabolism, water and food intake, as well as circadian rhythm, stress response or defences. The time window targeted in this experiment (postnatal period from day 12 to day 16) covers the ontogeny of the major neuronal circuits driving the regulation of food intake [17] and therefore is a period of high energy fuel demand by the brain and intense plasticity illustrated by neuronal migration, axon outgrowth and synapse formation [18].

2. Methods and materials

2.1. Animals and diet

All experiments were performed in accordance with the European Communities Council Directive of November 24, 1986, (86/609/ECC) regarding the care and use of animals for experimental procedures. All protocos were submitted and validated by Animal Care Local Committee of Pays de Loire (CREEA). Eight-week-old female and male Sprague–Dawley rats (Janvier, Le Genest Saint Isle, France) were maintained under controlled conditions (22°C, 12-h/12-h dark/light cycle) with free access to regular food containing 16 g protein per 100-g pellet (A04, Safe, Augy, France) and tap water. After 10 days of habituation, female rats were mated overnight with a male, and copulation was verified the next morning by the presence of spermatozoa in vaginal smears. From the day of conception, 26 pregnant dams were housed individually and were randomized to receive either a normal protein diet (control diet, C, containing 20% protein) for 14 of them or an isocaloric, low-protein diet (restricted diet, R, containing 8% protein) for 12 of them, as described previously [19] (Table 1). Diets were purchased from Arie Block BV (Woerden, the Netherlands) At birth, pups born from C and R mothers were randomly assigned to six C foster mothers or three R foster mothers so as to form litters of eight male pups for three experimental groups, CC, RC and RR, where the first letter depicts the maternal diet administered during gestation, and the second letter the maternal diet received by lactating dams during lactation. At postnatal day (PND) 12 and then at PND 16, eight pups from each group were euthanized.

2.2. Sample collection

Rats were rapidly euthanized between 9:00 and 11:00 AM by CO_2 inhalation. Blood was collected in heparinized tubes (Laboratories Léo SA, St. Quentin en Yvelines, France) and centrifuged at 2500*g* for 15 min at 4°C. After removing the brain from the skull, hypothalamus was dissected (according to Paxinos atlas coordinates −1.0 to −4.5 mm from bregma and 3 mm in depth, as previously described [20]) on an ice tray, weighted then snap-frozen in liquid nitrogen and stored at −80°C.

2.3. Biochemical analysis

Plasma leptin and insulin concentrations were determined with specific enzyme-linked immunosorbent assay (ELISA) kits (rat/mouse insulin ELISA kit and rat/mouse leptin ELISA kit; Linco Research, St. Charles, MO, USA).

2.4. Hypothalamus preparation for two-dimensional gel electrophoresis

Frozen hypothalamus aliquots of 30 mg were mechanically ground with beads (3 min at 30 000 shocks/s) and immediately treated with 1500 μl RP1 buffer of the Nucleospin RNA/protein kit containing β-mercaptoethanol according to the protocol supplied by the manufacturer (Macherey-Nagel, Hoerdt, France). Then, 350 μl of sample was eluted on Nucleospin RNA/protein column by addition of 350 μl of RP1 buffer and 350 μl of ethanol 70%. Then, 700 μl of protein precipitator was added to the column flow to precipitate protein. The protein pellet, collected by a first centrifugation (11 000*g* for 5 min at 4°C), was washed with 500 μl of 50% ethanol, then centrifuged again (at 11 000*g* for 1 min at 4°C), dried for 5–10 min at room temperature and then solubilized in 100 μl of lysis buffer (urea 7 M, thiourea 2 M, 3-[(3-cholamidopropyl) dimethyl-ammonio]-1-propanesulfonate 4%, dithiothreitol [DTT] 40mM, TritonX 100 1%, supplemented with a 1/100 dilution of a protease inhibitor cocktail [GE Healthcare, Orsay, France]). Contaminants and salts were eliminated by 2D-Clean-Up treatment according to the manufacturer's procedure (GE Healthcare), and the pellet of proteins was solubilized in 100 μl of lysis buffer with 2% immobilized pH gradient (IPG) buffer 3–10 (GE Healthcare). One aliquot was used for determination of protein concentration according to the Non Interfering Protein Assay (Agro-Bio, La Ferté Saint Aubin, France) using bovine serum albumin as standard. We verified that the presence of urea did not interfere with the protein assay.

2.5. Two-dimensional gel electrophoresis

Each run for the two-dimensional gel electrophoresis (2-DE) separation was carried out with all protein samples obtained from the three different groups of pups (CC, RC and RR) for stage at PND 12 and at PND 16. An amount of ~250 μg of the sample protein (~50 μl) was added to 200 μl of DeStreak solution (GE Healthcare) containing a trace of bromophenol blue (Biorad, Marnes La Coquette, France) and added with 0.5% IPG buffer, mixed and loaded to 13-cm-long ready-made Immobiline Drystrip gels

Table 1
Composition of the maternal experimental diets administered during gestation and/or lactation

	8% Protein (g/kg diet)	20% Protein (g/kg diet)
Proteins and amino acids		
Casein	90	220
Methionine	0.8	2.0
Carbohydrates		
Dextrose	681.7	551.5
Starch of corn	80.0	80.0
Lipids		
Soya oil	43.0	43.0
Fibers		
Cellulose	50.0	50.0
Vitamins and minerals mixture	50.5	49.5
Choline	4.0	4.0
Energy (kcal/kg diet)	3674.0	3722.7

(IPG) containing a wide linear gradient range pH 3–10 (GE Healthcare). Rehydration was performed overnight at room temperature, and isoelectrofocusing was performed on IPG Phor II (GE Healthcare) for 50 μA/IPG strip at 150 V for 2 h followed by 300 V for 3 h then 1500 V for 1 h and 5000 V for 11 h. Strips were equilibrated in buffer containing Tris 50 mmol/L (pH 8.8), urea 6 M, sodium dodecyl sulphate (SDS) 20%, glycerol 30%, DTT 64 mmol/L and a trace of bromophenol blue (Sigma-Aldrich, L'Isles d'Abeau, France), followed by a second incubation in the same buffer with the exception of DTT being substituted by iodoacetamide 135 mmol/L (Sigma-Aldrich), for 10 min, under gentle shaking. The equilibrated strips were transferred on top of a 12.5% SDS polyacrylamide gel electrophoresis (PAGE) (16×16×0.1 cm) and embedded in low melting agarose. Electrophoresis was performed at 10 mA/gel for 1 h followed by 20 mA/gel using a Rubby 600 SE system (GE Healthcare) until the dye reached the bottom of the gel. After fixation overnight in an aqueous solution of 50% ethanol and 2% orthophosphoric acid, the gels were incubated for 1 h in 2% orthophosphoric acid and sensibilised during 20 min in a solution of 17% ethanol, 15% ammonium sulphate and 2% orthophosphoric acid before the addition of 0.1% colloidal Coomassie blue G250 (Bio-Rad). After 3 days, the gel was destained by 2×10-min incubation in deionised water, followed by 10 min in 20% ethanol solution and then 10 min in deionised water. Colloidal Coomassie blue staining allows a narrow dynamic range, a good reproducibility and a good reliability for mass spectrometric (MS) analysis [21].

2.6. Image analysis

The gels were immediately scanned (16 bits/pixel in gray scale and 600-dots/inch resolution, i.e., 42.5 μm of resolution) using an Epson Perfection V750 PRO (Ozyme, Saint Quentin en Yvelines, France), and images were obtained with a digitalization software (Epson scan software, Ozyme). Raw images of the 2-DE gels were saved as TIF files and imported into the Image Master 2D platinum V6.0 analysis software (GE Healthcare). A total of 48 2-DE gels comprised the initial data set with two match sets constructed for the two stages of development at PND 12 and PND 16. For each match set, three submatch sets were built based on the pups groups: CC, RC and RR. There were between six and eight biological replicates corresponding to the hypothalamic proteins patterns of six to eight pups in each submatch sets. To accurately compare the measurements of spots in different gels, all gel images were cropped for keeping, exactly, the same area from the images that contain information of interest, and sensitivity parameters were controlled for the detection of approximately the same numbers of spots in each gel of the considered match set. Each gel underwent automatic spot detection and then manual spot editing, particularly in horizontal streaking, where some close spots might not be distinguished carefully. Saturated spots were excluded in order to work in the linear range of Coomassie blue staining. Then, the volume for a spot in each gel image was normalized by dividing its volume by the total volume of all the spots resolved in the gel (outliers being removed) to obtain a relative spot volume (expressed as % volume, [%vol]) in order to take into account variations due to protein loading and staining and make gels comparable. The gels with the most matched spots were defined as match-masters for each match set (PND 12 and PND 16) and used for automatic spot matching both within and between submatch sets, followed by manual fine editing matching when necessary. Only spots detected in a minimum of n-1 biological replicates from the three submatch sets were considered for differential analysis.

2.7. Data analysis

At first, we used a spot-by-spot approach (univariate analysis) using the nonparametric Kolmogorov–Smirnov test (included into the Image Master 2D platinum V6.0 analysis software; GE Healthcare) in order to detect matched spots showing statistically significant difference in their relative spot volume between two groups of pups (submatch sets: CC vs. RC, CC vs. RR and RC vs. RR) at the two stages (PND 12 and PND 16). The statistically significant difference was set at $P<.05$ and was evaluated by the Kolmogorov–Smirnov test statistic D, defined as the maximum distance between the empirical distribution functions of the two compared groups. If D was greater than a particular decision limit (critical value found in a Kolmogorov–Smirnov table for 5%, http://www.cons-dev.org/elearning/stat/Tables/Tab8b.html), there was a statistically significant difference between the distributions of the two groups. D was reported for each annotated spot, with their spot numbers and annotations, on Table 2 (and Supplemental Table 2) and Table 3 (and Supplemental Table 3) at PND 12 and PND 16, respectively. The variables, corresponding to the spots determined to be significantly different in the distribution of their relative volume using the Kolmogorov–Smirnov test, were log transformed, mean centered, scaled to unit variance and then introduced to multivariate analysis by using Simca-P+ software (version 12.0; Umetrics, Sigma Plus, Levallois-Perret, France). Principal component analysis (PCA), an unsupervised pattern recognition technique used in proteomic analysis [22], was performed to assess variation and expose any trends or outlying data. The supervised partial least-squares discriminant analysis (PLS-DA) was then performed to define the maximum separation between the three pups groups. The data were visualized by constructing principal component (PC) scores and loadings plots, where each point on the score plot represented an individual hypothalamus sample and each point on the loadings plot represented a single protein spot. The values of PC loadings reveal those 2D spots (variables) that are responsible for classification in the scores plots and are therefore potential biomarkers. The further away the variables are from the origin, the stronger their effect on discrimination. In the Western blot analysis, the data obtained from RC and RR hypothalamic extracts were compared with those of the CC group using the Kolmogorov–Smirnov test by using *R*.2.9.1 free software. The differences among pups' body weights were analyzed by Mann–Whitney U test, and plasma leptin and insulin concentrations data were first analyzed using two-way analysis of variance (ANOVA) with age and maternal diet as the main factors using Statview 5.0 (SAS Institute Inc., Cary, NC, USA). In all tests, $P<.05$ was considered significant.

2.8. Mass spectrometric analysis

Mass spectrometric analyses were conducted by the platform "Biopolymers-Interactions-Structural Biology" located at the INRA Centre of Nantes (INRA UR1268, F-44300 Nantes) (http://www.angers nantes.inra.fr/plateformes_et_plateaux_techniques/plateforme_bibs).

2.9. In-gel digestion

For identification, protein spots were manually excised from the gel. Gel pieces were destained for 30 min in 100 μl of a 25-mM ammonium bicarbonate solution and then for 45 min in 100 μl of a 25-mM ammonium carbonate/acetonitrile (vol/vol) solution. Cysteines were reduced with 10 mM DTT (Sigma Aldrich) in 25 mM ammonium carbonate for 1 h at 57°C followed by alkylation with 55 mM iodoacetamide (Sigma-Aldrich) in 25 mM ammonium carbonate for 45 min at room temperature. Spots were subsequently washed with 25 mM ammonium carbonate and then with 12.5 mM ammonium carbonate/25% acetonitrile to remove excess reagents. Ten microliters of 15 ng/μl trypsin (sequencing grade modified trypsin from PROMEGA ref. V5111, Charbonnières-les-Bains, France) in 25 mM ammonium carbonate was added to the gel plug, and incubation was performed at 37°C overnight. The tryptic digestion was stopped by addition of 1 μl of 10% formic acid, and hydrolysates were stored at −20°C until analysis.

2.10. Matrix-assisted laser desorption/ionization–MS analysis

Protein identification was first attempted by "peptide mass fingerprint" approach using matrix-assisted laser desorption/ionization (MALDI)–time-of-flight (TOF) MS. Analyses were performed with a MALDI LR instrument equipped with a conventional laser at 337 nm (Micromass-Waters, Manchester, UK). One microliter of the sample was mixed with 1 μl of the matrix preparation (2.5 g/L α-*cyano*-4-hydroxycinnamic acid [Sigma-Aldrich], 2.5 g/L 2,5-dihydroxy benzoic acid [Sigma-Aldrich] in a 4.5-mM ammonium phosphate solution containing 70% [vol/vol] acetonitrile, 0.1% [vol/vol] trifluoroacetic acid and 0.02 pmol/μl of glu-fibrinopeptide [Sigma-Aldrich] for internal calibration) and deposited onto the MALDI sample probe. Mass accuracy of approximately 75 ppm was achieved with internal calibration (lock-mass ion at 1570.677 m/z corresponding to the monoprotonated species of the glu-fibrinopeptide or at 2211.105 m/z corresponding to an autolysis peptide from trypsin). Databank searches were performed as described below. When proteins remained unidentified at this stage or for a further validation of the identifications, a liquid chromatography–tandem mass spectrometry (LC-MS/MS) analysis was done.

2.11. LC-MS/MS analysis

Nanoscale capillary LC-MS/MS analyses of the digested proteins were performed using a Switchos-Ultimate II capillary LC system (LC Packings/Dionex, Amsterdam, the Netherlands) coupled to a hybrid quadripole orthogonal acceleration time-of-flight mass spectrometer (Q-TOF Global, Micromass/Waters, Manchester, UK). Chromatographic separation of peptide samples (5 μl loaded on column) was conducted on a reverse-phase capillary column (Pepmap C18, 75-μm i.d., 15-cm length, LC Packings) at a flow rate of 200 nL min^{-1}. The gradient consisted of a linear increase from 2% to 40% of acetonitrile in 50 min followed by a rapid increase to 50% of acetonitrile within 10 min. The mass spectrometer was operated in the positive-ion mode. Mass data acquisitions used the so-called "data dependent acquisition" mode: The MS data were recorded for 1 s on the mass-to-charge (m/z) range 40–-1500, after which the three most intense ions (doubly or triply charged ions) were selected and fragmented in the collision cell (MS/MS measurements).

2.12. Protein identification–databank searching

Raw data were processed using the Protein Lynx Global Server software (version 2.1; Micromass/Waters, Manchester, UK). Protein identification was performed by confronting the collected MALDI-MS and/or LC-MS/MS data against the Uniprot sequence databank (http://www.expasy.ch/sprot/), restricted to the species *Rattus norvegicus*. Databank searches were performed using MASCOT server 2.2 (Matrix Science). Mass tolerance was set at 100 ppm for parent ions (MS mode) and 0.3 Da for fragment ions (MS/MS mode); one missed cut per peptide was allowed; fixed modification of cysteines by iodoacetamide and variable modification of methionine by oxidation were considered. A significant P value threshold for protein validation was set at .05.

Table 2
Hypothalamus protein alterations in pups in response to maternal protein restriction at PND 12

Spot number	Accession number Swiss-Prot/TremBL	Protein name (abbreviations used in text)	Gene name	Quantitative change expressed as the ratio of abundances (Kolmogorov test with the *D* value for $P<.05$)		
				RC vs. CC	RR vs. CC	RR vs. RC
		A. Proteins involved in oxidative stress				
8944	P62260	14-3-3 protein epsilon	Ywhae	1.90 (0.857)		
8944	P63102	14-3-3 protein zeta/delta	Ywhaz	1.90 (0.857)		
8944	P68255	14-3-3 protein theta	Ywhaq	1.90 (0.857)		
8944	P61983	14-3-3 protein gamma	Ywhag	1.90 (0.857)		
8944	P68511	14-3-3 protein eta	Ywhah	1.90 (0.857)		
8797	Q6DGG0	40 kDa peptidylprolyl-*cis-trans*-isomerase (Pin1)	Ppid			1.50 (0.714)
8514	O35814	Stress-induced-phosphoprotein 1 (Stip1)	Stip1			2.10 (0.714)
9020	Q9ZOV6	Thioredoxin-dependent peroxide reductase (PrdX 3)	Prdx3			2.80 (0.830)
		B. Proteins involved in growth and energy metabolism				
8652	P04764	Alpha enolase (Eno1)	Eno1		1.25 (1)	
8883	Q45QL2	Guanine nucleotide binding protein subunit 4 (Gnb4)	Gnb4		2.13 (0.833)	
8490	P08461	Dihydrolipoyllysine-residue acetyltransferase component of pyruvate dehydrogenase complex (E_2PDH)	Dlat	−3.84 (0.714)		
8708	O88267	Acyl-coenzyme A thioesterase I (Acot1)	Acot1			2.77 (0.857)
8735	P02651	Apolipoprotein A-IV (Apo A-IV)	Apoa4			2.20 (0.714)
8797	P09117	Fructose biphosphate aldolase C (AldoC)	AldoC			1.50 (0.714)
8883	O88989	Malate dehydrogenase cytoplasmic	Mdh1		2.13 (0.833)	
8797	Q5XI22	Acetyl CoA acetyltransferase (Acat2)	Acat2			1.50 (0.714)
8797	Q64559	Acyl CoA thioester hydrolase (Acot7)	Acot7			1.50 (0.714)
8490	Q6P7A9	Lysosomal alpha-glucosidase precursor	Gaa	−3.84 (0.714)		
		C. Proteins involved in neuronal migration, axon growth and guidance				
8478	P47942	Dihydropyriminidase related protein 2 (DRP2)	Dpysl2			1.89 (0.714)
8507						1.55 (0.857)
8505						1.7 (0.714)
8490				−3.84 (0.714)		
8551	Q62952	Dihydropyriminidase related protein 3 (DRP3)	Dpysl3			1.25 (0.714)
8513					2.94 (0.833)	
8520	Q9JMG8	Dihydropyriminidase related protein 5 (DRP5)	Dpysl5			2.42 (0.714)
8514	Q9JHUO					2.10 (0.714)
8576	P31000	Vimentin	Vim			−1.8 (0.714)
8481						1.53 (0.714)
8621	Q6AYH5	Dynactin subunit 2	Dctn2	1.48 (0.714)		
8658	A9CM90	Actin-related protein 3 (ARP3)	Arp3	−2.4 (0.714)		
8635	AOJN25	Microtubule-associated protein 2 (MAP2)	Mapt			3.57 (0.83)
9063	P37377	Alpha-synuclein (Snca)	Snca			3.05 (0.714)
8501	Q6P502	T-complex protein (TCP-I)	Cct3			2.92 (0.714)
8944	Q91XN7	Tropomyosin alpha isoform (Tpm1)	Tpm1	1.90 (0.857)		
8944	A2RUW1	Toll interacting protein (Tollip)	Tollip	1.90 (0.857)		
8490	O89046	Coronin-1B	Coro1B	−3.84 (0.714)		

Spots numbers with corresponding Swiss-Prot database accession number, the protein name, the corresponding gene name and the modulation level (quantitative change or ratio) are shown. The quantitative change was evaluated by the maximum ratio of abundances between the lower limit of one of the other classes and the upper limit of the current class. For a quantitative change less than 1, the ratios are inversed and are preceded by a minus sign. The statistically significant variability in the expression pattern of the protein spots was set at $P<.05$. The Kolmogorov–Smirnov test statistic *D* value was defined as the maximum distance between the empirical distribution functions of the two compared groups.

2.13. Validation of protein identifications

For MALDI-MS, proteins having MASCOT scores above the significance threshold ($P<.05$) were validated when their sequence coverage was above 56%. For MS/MS experiments, proteins were identified with a minimum of two MS/MS spectra matching the databank sequence with individual MASCOT ion scores above the significance threshold ($P<.05$) (individual ion scores of more than 26). Results were validated and exported in an analytical report using the OVNIp software developed by INRA Nantes (Tessier et al., personal communication).

2.14. Gene Ontology annotations

The proteins identified in this study were functionally categorized based on universal Gene Ontology (GO) (**www.geneontology.org/**) annotation terms of their compartment localization and their biological process.

2.15. Western blotting

Hypothalamic proteins pellet collected after treatment by Nucleospin RNA/protein kit (Macherey-Nagel, Hoerdt, France) were then solubilized in Tris–HCl 10 mM pH 7.5, 1% SDS and protease inhibitor cocktail. Protein concentration was quantified by the BCA protein assay kit (Pierce, Thermo Scientific, Rockford, IL, USA) following the manufacturer's instructions. Fifteen micrograms of hypothalamic protein extracts was separated on 12% (wt/vol) SDS-Page and transferred to nitrocellulose membranes. The membranes were blocked for 1 h at room temperature in blocking buffer (20 mM Tris–HCl, pH 7.5, 135 mM NaCl, 0.1% [vol/vol], Tween 20 [TBST] containing 5% dried fat-free milk), washed four times in TBST and then incubated with the primary antibodies overnight at 4°C. Primary antibodies were rabbit anti-CRMP2 polyclonal antibodies diluted 1/1000 (vol/vol) (Abcam, Cambridge, England), rabbit anti-CRMP5 polyclonal antibodies diluted 1/2000 (vol/vol), rabbit anti-aldolase C polyclonal antibody diluted 1/1000 (vol/vol) (Cell Signaling Technology, Ozyme, St-Quentin-en-Yvelines, France) and rabbit anti-aminoacylase-1 polyclonal antibodies diluted 1/400 (vol/vol) (Santa-Cruz Biotechnology Inc., Santa Cruz, CA, USA) in TBST containing 5% bovine serum albumin. The membranes were washed four times with 1% Tween 20/TBS and then probed for 1 h with secondary goat peroxidase-conjugated antibody (1:10 000 vol/vol) anti-rabbit IgG (Jackson Immuno Research, West Grove, PA, USA). Signal was revealed using enhanced chemiluminescence reagents (Uptilight US HRP WB substrates, Uptima, Interchim, Montluçon, France). Blots were scanned on the G:Box Chemi XL (Syngene, Ozyme, St-Quentin-en-Yvelines, France). A semiquantitative analysis based on densitometric values (arbitrary units) was performed by GeneTools software (Syngene, Division of Synoptics Ltd, Cambridge, England).

Table 3
Hypothalamus protein alterations in pups in response to maternal protein restriction at PND 16

Spot number	Accession number Swiss-Prot/TremBL	Protein name (abbreviations used in text)	Gene name	Quantitative change expressed as the ratio of abundances (Kolmogorov test with the *D* value for $P<.05$)		
				RC vs. CC	RR vs. CC	RR vs. RC
		A. Proteins involved in oxidative stress				
3461	P62260	14-3-3 protein epsilon	Ywhae	1.39 (0.708)		
3492	P63102	14-3-3 protein zeta/delta	Ywhaz		−2.34 (0.750)	
3525	P20788	Cytochrome b-c1 complex subunit Rieske (Bcs1L)	Uqcrfs 1	2.90 (0.708)		
3533	Q9Z0V6	Thioredoxin-dependent peroxide reductase (PrdX3)	Prdx 3		−1.55 (0.750)	
3286	Q9BV20	Translation factor eIF-2B subunit alpha (eIF2B)	eIF2B		−2.05 (0.750)	
3286	Q9Z254	PDZ domain-containing protein GIPC1	Gipc1		−2.05 (0.750)	
3544	B0BNE6	NADH dehydrogenase ubiquinol iron–sulphur protein (Ndufs8)	Nudfs8	−1.60 (0.750)		
3545					−1.8 (0.875)	
		B. Proteins involved in energy and protein metabolism				
2942	P02770	Serum albumin	Alb		−1.77 (0.875)	−2.2 (1)
2946					−1.67 (0.750)	−2.1 (0.830)
3400	O88989	Malate dehydrogenase (MDH)	Mdh1	−1.54 (0.750)		
3461	Q6MG61	Chloride intracellular channel 1 (Clic1)	Clic1	1.39 (0.708)		
3065	Q08651	D-3-phosphoglycerate dehydrogenase (GAPDH)	Gapdh			−1.87 (0.708)
3276				−1.54 (0.708)		
3297	P09117	Fructose biphosphate aldolase C (AldolC)	AldoC			1.36 (0.750)
3354	P42123	L-Lactate dehydrogenase B chain (LDH)	Ldhb	−1.32 (0.750)		
3536	P04639	Apolipoprotein A-I (Apo A-I)	Apoa 1		−2.31 (1)	
3544	Q6P7Q4	Lactoylglutathione lyase (glyoxalase 1)	Glo1	−1.60 (0.750)		
3545					−1.8 (0.875)	
3589	P55053	Fatty-acid binding protein, epidermal (Fabp5)	Fabp5		−4.28 (0.875)	
3506	P60901	Proteasome subunit alpha type 6	Psma6		−1.78 (0.750)	
3544	P28073	Proteasome subunit beta type 6	Psmb6	−1.60 (0.750)		
3545					−1.8 (0.875)	
3195	P04182	Ornithine aminotransferase (OAT)	Oat	−1.63 (0.708)		
3235	Q6AYS7	Aminoacylase-1A (Acy1)	Acy1	−2.15 (0.750)		
3400	O35331	Pyridoxal kinase (Pdxk)	Pdxk	−1.54 (0.750)		
		C. Proteins involved in neuronal migration, axon growth and guidance				
2993	Q9JHU0	Dihydropyriminidase related protein 5 (DRP5)	DpysI5	−1.57 (0.750)		
3204	Q01986	Mitogen-activated protein kinase-kinase 1 (MAPKK1)	Map2k1	−2.10 (0.750)		
3195				−1.63 (0.708)		
3195	Q4KLK4	Actin-related protein 1 homolog B (Arp1)	Arp 1	−1.63 (0.708)		
3195	P85515	Alpha-centractin	Actr1a	−1.63 (0.708)		
3211	P60711	Actin cytoplasmic 1	Actb			−1.9 (0.708)
3204				−2.10 (0.750)		
3211	Q5XID2	TAR DNA binding protein (TDP-43)	Tardbp			−1.9 (0.708)
3204				−2.10 (0.750)		
3211	Q4FZT2	Protein phosphatase methylesterase 1 (fragment)	Ppme1			−1.9 (0.708)
3091	Q61553	Fascin	Fscn1	−1.7 (0.750)		
3533	O35791	RhoA	Rhoa		−1.55 (0.750)	
		E. Others				
3492	Q64361	Latexin	Lxn		−2.34 (0.750)	

Spots numbers with corresponding Uni-Prot database accession number, the protein name, the corresponding gene name and the modulation level (quantitative change or ratio) are shown. The quantitative change was evaluated by the maximum ratio of abundances between the lower limit of one of the other classes and the upper limit of the current class. For a quantitative change less than 1, the ratios are inversed and are preceded by a minus sign. The statistically significant variability in the expression pattern of the protein spots was set at $P<.05$. The Kolmogorov–Smirnov test statistic *D* value was defined as the maximum distance between the empirical distribution functions of the two compared groups.

3. Results

3.1. Body weights and biochemical parameters of IUGR pups

In this study, at birth, R pups presented a 12% lower ($P<.05$) birth weight compared to C pups. Then, RC and RR pups had, respectively, a 12% (NS) and 33% lower ($P<.001$) body weight than CC pups at PND 12 and 7% higher ($P<.05$) and 36% lower ($P<.001$) body weight than CC pups at PND 16. RC pups showed an accelerated weight gain (34%, $P<.01$ CC vs. RC) during the first week of life. Plasma leptin and insulin were modulated by maternal nutrition at PND 12 and PND 16, as represented in Fig. 1. Plasma leptin of the same RR rats were reported to be significantly reduced compared with CC ($P<.001$) and RC ($P<.001$) rats at PND 12 (Fig. 1A). Plasma insulin levels in RR rats were half ($P<.05$) the value of CC rats at PND 12 and a quarter of the value of CC ($P<.001$) and RC ($P<.01$) rats at PND 16 (Fig. 1B) (as described in our previous work [24]).

3.2. Normal hypothalamic proteome changes between PND 12 and PND 16 in control rats

To analyze the physiological changes in hypothalamus proteome associated with normal postnatal brain development, total protein extracts of the whole hypothalamus from CC rats at PND 12 (Fig. 2) and PND 16 (data not shown) were separated by 2-DE. Protein patterns increased in complexity from PND 12 to PND 16 ($P=.004$, Mann–Whitney test), suggesting an increase in the number of proteins with the age: an average of 444±83 and 595±64 protein spots were detected at PND 12 ($n=6$) and 16 ($n=7$), respectively.

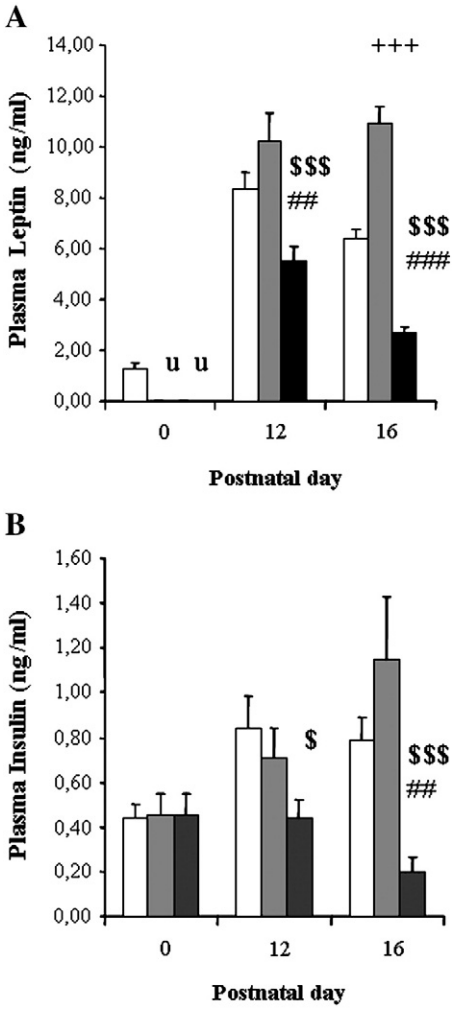

Fig. 1. (A) Plasma leptin concentrations in CC, RC and RR pups at PND 12 and 16; (B) plasma insulin concentrations in CC, RC and RR pups at PND 12 and 16: CC group (open bars), RC group (gray bars) and RR group (black bars). Data were analyzed by an ANOVA test. Values are means±SEM; n=6–8 per group. +++, P<.001 for RC vs. CC; $, P<.05; $$, P<.01; $$$, P<.001 for RR vs. CC; ###, P<.001 for RC vs. RR; u: undetectable.

3.3. Maternal protein restriction during gestation only (RC) or during gestation and lactation (RR) induces differential changes in hypothalamus proteome

About 70% of the spots were matched between all the gels of the submatch sets corresponding to the three pup groups at the two stages. According to the total number of spots, only the RR group had a significant (P=0.01, Mann–Whitney test) increase in the complexity of the protein patterns between the two stages of development. The comparison between the proteomes of the three groups of pups revealed 22 and 25 spots significantly different at, respectively, PND 12 and PND 16 that were correctly annotated and corresponded to, respectively, 30 (PND 12, Table 2) and 31 (PND 16, Table 3) different genes, as we identified two or more overlapping proteins by LC-MS/MS in 22% of spots at PND 12 and 61% of spots at PND 16. We observed a greater number of spots significantly different between the CC and RC groups at PND 16 (12 spots) than at PND 12 (4 spots) and between the CC and RR groups (4 spots for PND 12 vs. 9 for PND 16). At the opposite, the number of spots significantly different between RR and RC decreased from 15 spots at PND 12 to 6 spots at PND 16 (Tables 2 and 3).

To obtain an overview of the changes induced by perinatal protein restriction in pup hypothalamic proteome, the identified proteins were linked to at least one GO annotation category and, more precisely, to 7 subcellular compartments (Fig. 3A) and 13 biological processes (Fig. 3B). The majority of the identified proteins are intracellular proteins (95%), among which most are distributed in the cytoplasm (76% at PND 12 and 77% at PND 16), mitochondrion (20% at PND 12 and 27% at PND 16) and cytoskeleton (17% at PND 12 and 19% at PND 16). Fig. 3B showed the over-representation in the biological process category of GO terms related to “intracellular signalling cascade” (24%–13%) and “carbohydrate metabolic process” (15%–13%) at PND 12 and PND 16. In this later stage, three other classes were major: “the nervous system development” (14%), the “protein metabolic process” (12%) and the “response to oxidative stress” (12%).

3.4. Selection of the proteins which allowed the discrimination between the three groups (CC, RC and RR) at the two stages of development

The 47 significantly different spots observed at PND 12 and 16 were submitted to multivariate analysis. The unsupervised PCA provided a sharp separation between 2-DE of the three pup groups, with 57% of the total variation for PND 12 (Fig. 4A) and 42% for PND 16 (Fig. 4B) explained by the first two principal components. We could note one RC pup and one RR pup that were above the critical limit of the 95% Hotelling's T^2 control chart (95% confidence region) as represented by the ellipse on the PCA score plots at, respectively, PND 12 and PND 16. However, these outliers disappeared in the supervised PLS-DA model. The PLS-DA score plots showed three clusters of 2-DE patterns, with overall similar protein expression characteristics, which did not overlap particularly at PND 16. The PLS-DA loading plots allowed the identification of proteins which were the most predictive for the differences between the three groups. Fig. 4 depicts score (Fig. 4C at PND 12 and Fig. 4D at PND 16) and loading (Fig. 4E at PND 12 and Fig. 4F at PND 16) plots for the first two principal components (PC1 and PC2) which explained, respectively, 45% and 8% at PND 12 and 28% and 12% at PND 16 of the total variability. Along PC1, the RR group was sharply separated at PND 12 from the RC and CC groups, whereas at PND 16, a good separation was observed for all the three groups. The PC2 axis clearly discriminated the CC group from the two other groups at PND 12, whereas it was the RC group which was clearly separated from the two other groups at PND 16. According to the corresponding loading plots along PC1 and PC2, six proteins involved in neuronal migration and axon guidance (the dihydropyrimidinase related protein 5 and 2 or DRP5 and DRP2, the actin-related protein 3 or ARP3, the microtubule-associated protein 2 or MAP2, the brain-specific alpha-synuclein or Snca and the T-complex protein or TCP-I), three in energy metabolism (the acyl-CoA thioesterase I or AcotI, the dihydrolipoyllysine-residue acetyltransferase, a mitochondrial component [E2] of a pyruvate dehydrogenase complex [E_2PDH] and the brain-specific alpha-enolase or EnoI) presented a larger contribution to discriminate the RC and RR groups at PND 12, whereas one protein involved in redox regulation (14-3-3 protein epsilon) discriminated clearly the CC and RC groups. At PND 16, three oxidative stress proteins (the 14-3-3 protein zeta, the translation factor eiF-2B subunit alpha and the thioredoxin-dependent peroxide reductase [PrdX 3]) discriminated clearly RR and CC groups, whereas three proteins involved in energy metabolism (apolipoprotein A1 or Apo A-I, one isoform of serum albumin and epidermal fatty-acid binding protein or Fabp5) and two proteins involved in neurogenesis (actin and mitogen-activated protein kinase-kinase [MAPKK1], involved in signal transduction pathway) contributed to the three groups' discrimination. The oxidative stress marker (cytochrome bc1 complex or Bcs1L) and the aminoacylase (Acy1) involved in protein metabolism discriminated preferentially the RC group. Among these proteins, one displayed an overlapping expression in spots # 3461, with the 14-3-3 protein epsilon form as major component and the chloride intracellular channel 1 (Clic1) as minor component.

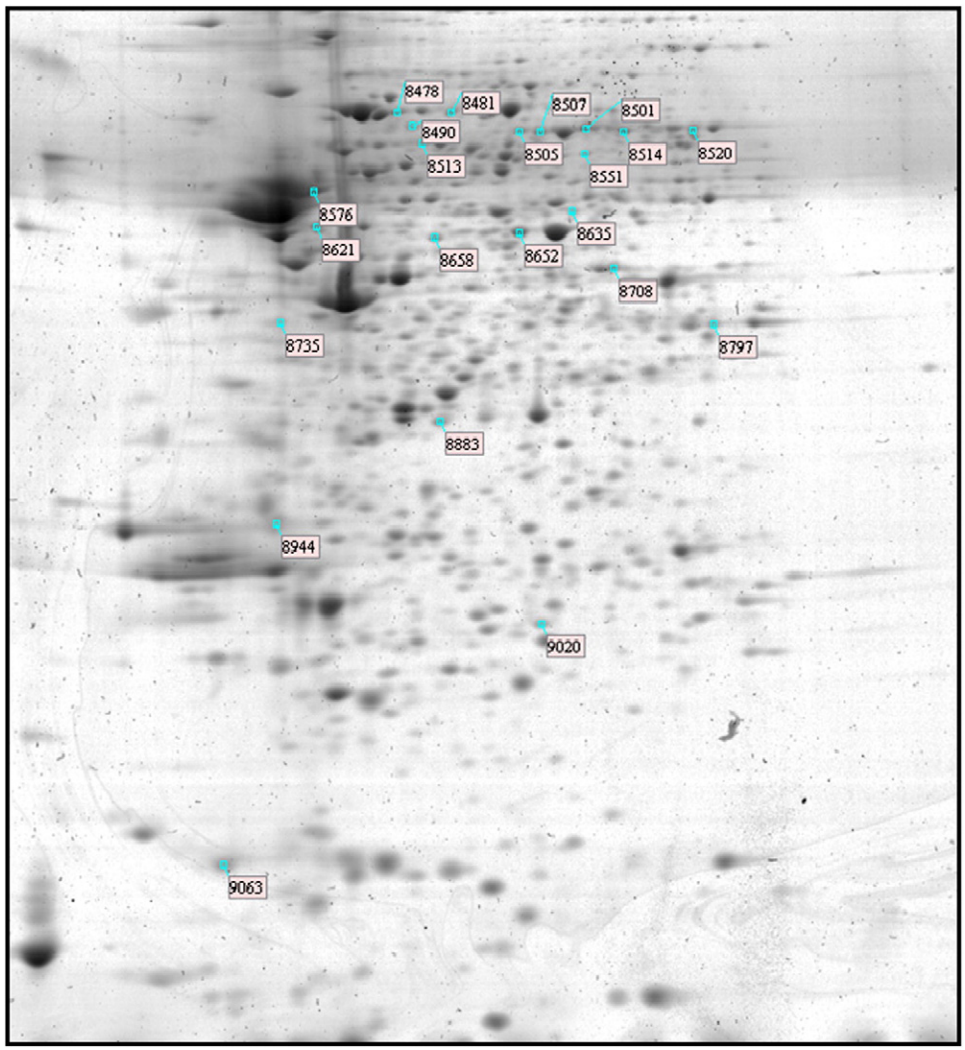

Fig. 2. Overview of hypothalamic proteins altered in response to perinatal protein restriction at PND 12. Total proteins extracted from the whole hypothalamus of pups were separated by 2-DE, according to their isoelectric point (pI) in the first dimension and to their molecular weight (Mw) in a second dimension. The proteins' 2-D gel images were visualized by Coomassie blue staining. The highlighted spots correspond to differentially expressed proteins according to the statistical analysis (Kolmogorov test, $P<.05$) in RR and RC pups compared to CC pups and analyzed by MALDI-TOF MS and/or LC-MS-MS. Identification of all proteins is depicted in Tables 1 and 2 for PND 12 and PND 16, respectively.

3.5. Protein validation by Western blot

Because it is essential for proteomics to provide accurate and reproducible results, changes in abundance of two proteins representative of neuronal signalling and two proteins representative of metabolism were further validated by the means of Western blot analyses. We confirmed that DRP2 (*P* value .0186 and .0001) and DRP5 (*P* value .0001 and .0003) exhibited, by Western blot analyses, a greater abundance in hypothalamic tissue of RR groups vs. RC and CC groups, respectively, at PND 12 (Fig. 5). Aldolase C was increased in RR groups compared to RC group (but not significantly) at PND 12, whereas aminoacylase I had lower abundance in RC group (*P* value .0286) compared to CC and RR groups at PND 16 by Western blot analyses (Fig. 5).

4. Discussion

The current study is the first systematic report on the changes occurring in the proteome of the developing hypothalamus in infant rodents subjected to IUGR, followed either by extrauterine growth retardation (RR group) or a rapid catch-up growth (RC group), compared to pups with normal growth during gestation and lactation (CC group). By comparing the hypothalamic proteome of these rats, we showed that both the development during gestation and the velocity of growth after birth had an impact on the abundance of enzymes of carbohydrate and fatty acid metabolism, proteins involved in oxidative stress and in neurodevelopment.

In our experiment, we obtained IUGR pups with significantly lower birth weight compared to CC pups. In a previous experiment, we demonstrated that RR pups submitted to a prolonged protein restriction until weaning displayed catch-up body weight gain from weaning onwards (+153% and+149% [$P<.01$] from PND 21 to PND 260 compared to CC and RC, respectively) [23]. Therefore, the down-regulation of plasmatic leptin and insulin in RR pups was previously shown to parallel an important immaturity of the hypothalamus [24]. In addition, we assumed that the changes we observed in the proteome of RC and RR pups could be attributed to the quantity of milk that pups received after birth since protein restriction of mother's diet during lactation has no effect on milk composition but on milk production that is reduced [25]. At PND 16, pups opened their eyes and started to nibble at food pellet of their mother's diet that was different between RR and RC–CC groups. However, the pieces of food eaten were negligible compared to milk intake.

In the present study, the number of differentially expressed proteins in the hypothalamus between the three groups was of the

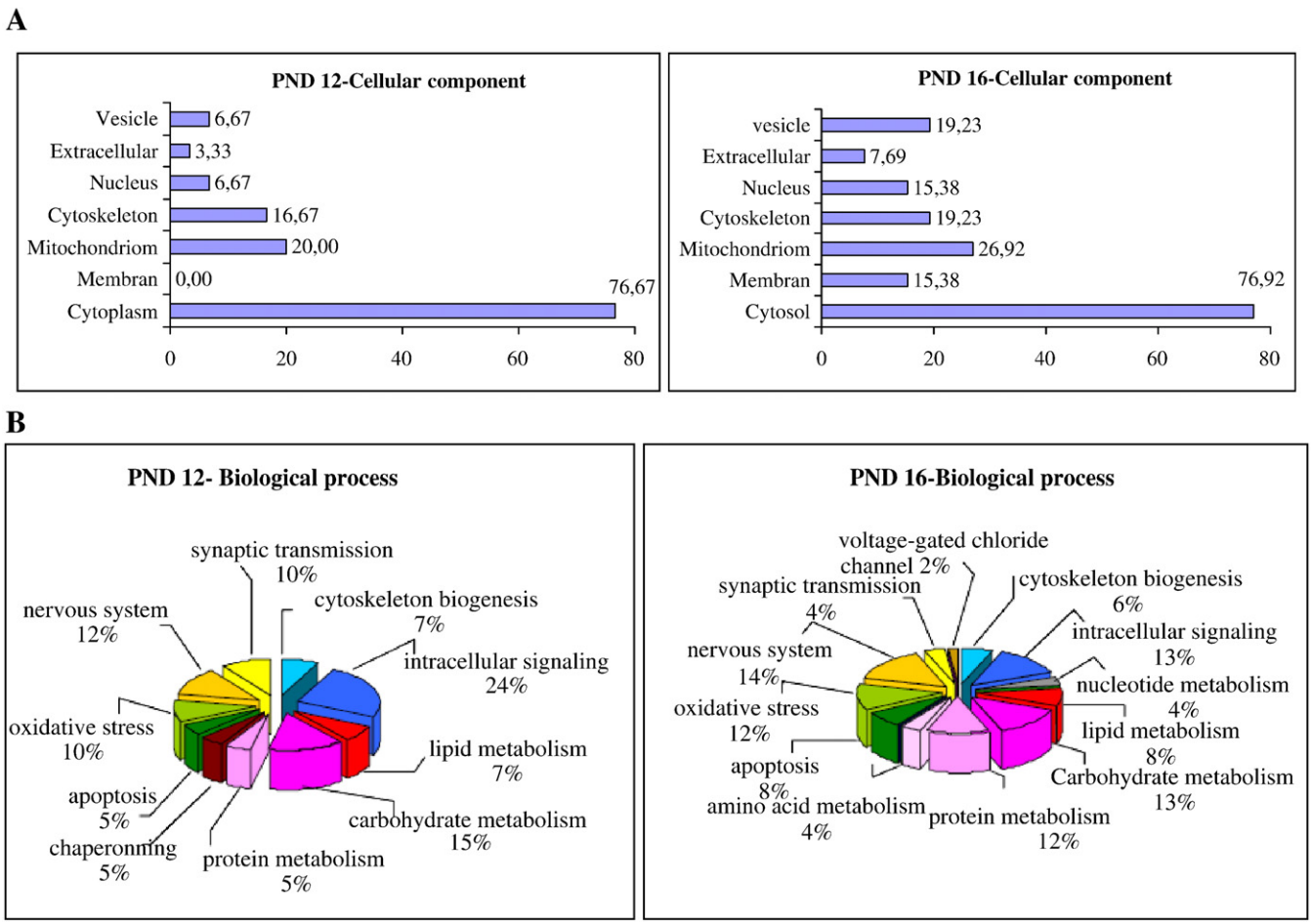

Fig. 3. Distribution of the identified maternal protein restriction-related hypothalamic proteins among various cellular components (bar charts, A) and biological processes (pie charts, B) at PND 12 and PND 16.

same magnitude than those previously observed in other IUGR models [26,27]. The number of spots for which we identified more than two overlapping proteins (20%), a well-known limitation of 2-DE-based separation methods [28], fits with two proteomic analyses of mouse cerebral cortex [29] and rat inferior colliculus and cerebellum [30]. A considerably higher number of MS/MS matched peptides and a higher MASCOT score often indicate one protein as the major component of a spot (these data are detailed on supplemental Table 2 and Table 3). Consequently, we assumed that an increase in relative volume of the spot was mainly due to higher abundance of this protein. However, if overlapping proteins belong to the same functional group, such as the five different 14-3-3 proteins in spot # 8944, it is likely that the whole group contributed to a higher % volume. Based on these considerations, limited information on differently expressed proteins can be assessed from spots with overlapping proteins [29,30]. We focused our discussion on the proteins that contribute the best to the discrimination of the groups and proteins involved in energy metabolism.

According to the hierarchical organization issued from the GO analysis of the 2D gel data, most of these proteins belong to the functional categories: oxidative stress, cell signalling involved in cell maintenance and metabolism regulation and neuronal development. Globally, at PND 12, a high number of protein spots with a differential abundance between both IUGR groups was related to neuronal development. These proteins were overexpressed in the IUGR pups maintained in protein restriction compared to the IUGR with rapid catch-up growth, suggesting discordance in brain maturation between IUGR pups that is in accord with our previous findings [20]. At the later stage, the key proteins presenting a differential abundance between both IUGR groups were mostly related to energy metabolism pathways, and the majority of these proteins were down-deregulated in the two groups of IUGR pups compared to control pups. In addition, the growth velocity of the IUGR pups modulated the deregulation of these pathways, as the prolonged protein restriction of IUGR pups significantly down-regulated some proteins involved in glycolysis and/or lipid metabolism.

4.1. Proteins involved in oxidative status

Emerging data suggest that oxidative stress and mitochondrial dysfunction may play critical roles in the individuals who were growth retarded at birth [31,32]. Previous studies demonstrated impaired oxidative phosphorylation in hepatic mitochondria [33] or in skeletal muscle [34] in a model of IUGR rats, and deregulated cellular redox status in small intestine, liver and skeletal muscle of neonatal IUGR piglets [27]. Rapid postnatal growth during lactation has been previously associated with markers of oxidative damage [9]. In the present study, the fact that IUGR followed by catch-up growth (RC group) down-regulated Bcs1L at the later stage of development is fully consistent with the decrease in the activity of cytochrome C oxidase (complex IV) measured in neonatal rat pups submitted to low-protein diet during gestation [35]. Bcs1L is involved in the complex III of the mitochondrial oxidative phosphorylation system (OXPHOS) tightly coupled to ATP generation and reactive oxygen

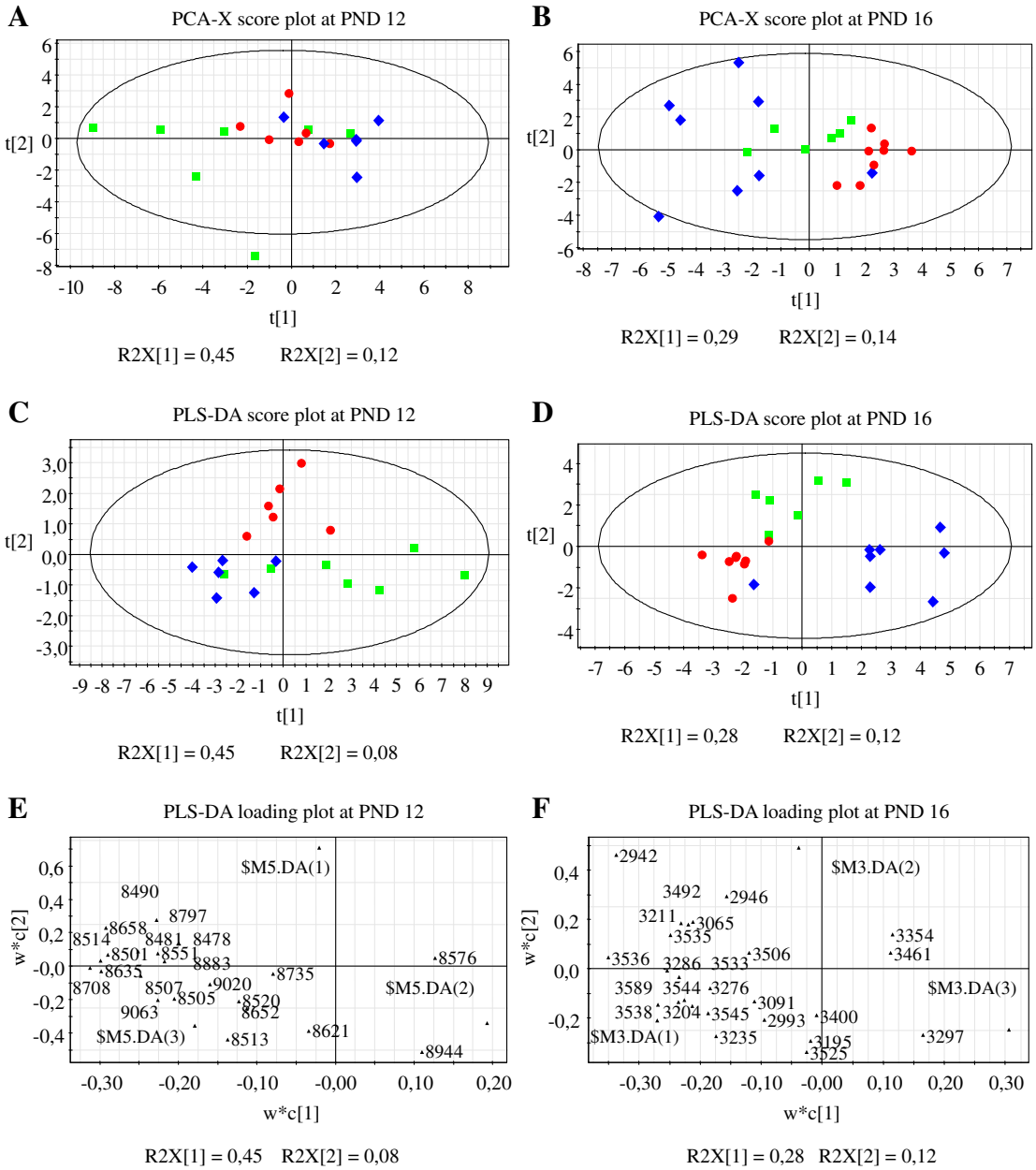

Fig. 4. Score scatter plots of PCA (A and B) and PLS-DA (C and D) (CC pups, red dot; RC pups, green box and RR pups, blue diamond); loading plots (E and F) of variables for the two components of PLS-DA for RR group at, respectively, PND 12 and PND 16. The ellipse in the two-dimensional score plot is the 95% confidence region (Hotelling's T^2 range). Multivariate analysis was conducted on all 19 hypothalamic protein samples from six CC, seven RC and six RR pups at PND 12 using 22 differentially expressed proteins and on all 22 hypothalamic protein samples from eight CC, six RC and eight RR pups at PND 16 using 25 differentially expressed proteins.

species (ROS) production [36]. The decrease of another partner of the mitochondrial complex I, the Nduf8 [37], in both IUGR pups at PND 16 is in agreement with alteration in mitochondrial complex system in response to protein restriction *in utero*. Reactive oxygen species have been proposed to function as signalling molecule in brain nutrient sensing [38,39]. So, it would be pertinent to measure OXPHOS functionality as well as ATP and ROS production in the hypothalamus of our RC pups. Three other proteins of the cellular redox machinery were also deregulated by perinatal protein restriction, which is in agreement with oxidative damage. The 14-3-3 proteins, involved in the regulation of most cellular processes (redox-regulation, mitochondrial import, protein trafficking and metabolism, signal transduction) [40], were up-regulated by rapid catch-up growth (RC) at both stages of development, whereas they were down-regulated by slow postnatal growth (RR) at PND 16 compared to CC. At PND 16, the PrdX 3, a complete peroxidase redox system similar to glutathione [41,42], was down-regulated in the RR group compared to CC. Taken together, our findings could suggest an adaptive mechanism in our RR and RC pups to dissipate oxidative stress in response to an adverse intrauterine milieu itself modulated by the postnatal growth velocity and by the stage of development during this critical period of the hypothalamus ontogeny.

4.2. Proteins involved in energy metabolism

Alterations of the intrauterine milieu associated to the growth pattern seemed to have an impact on the brain energy metabolism in the offsprings. In a previous piglet model with maternal protein

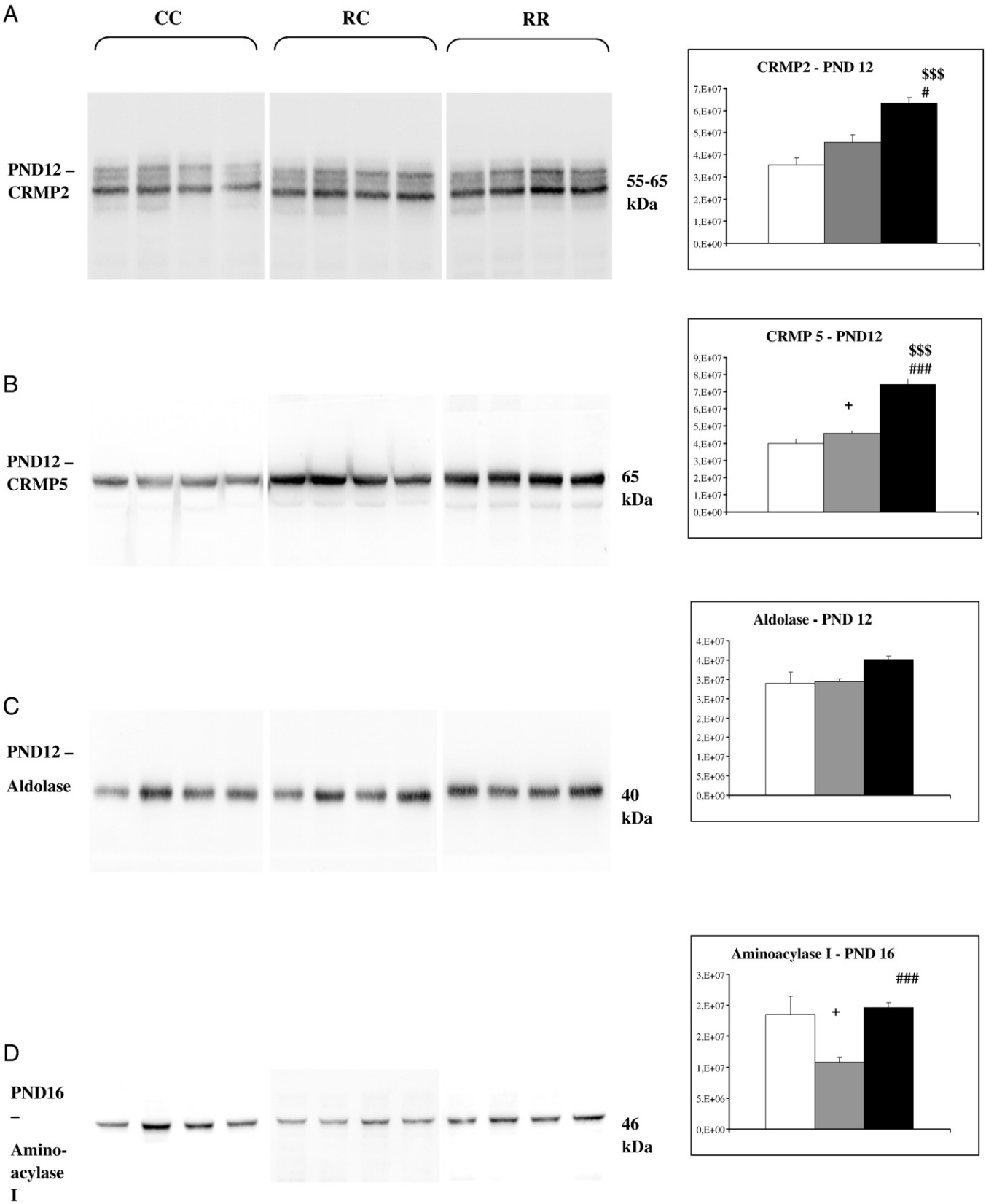

Fig. 5. Western blot analysis of CRMP 2 (A), CRMP5 (B) and aldolase C (C) expression in the hypothalamus of the three groups of rats at PND 12 and of aminoacylase 1 (D) expression at PND 16. Hypothalamic extracts were submitted to one-dimensional SDS-PAGE, followed by immunoblots with specific antibodies. Representative Western blots are shown together with densitometric analysis of protein bands of interest: CC group (white bars), RC group (gray bars) and RR group (black bars). Data were analyzed by a Kolmogorov test. Values are means (arbitrary units)±SEM; n=6–8 per group. +++, P<.001 for RC vs. CC; $, P<.05; $$, P<.01; $$$, P<.001 for RR vs. CC; ###, P<.001 for RC vs. RR.

restriction during gestation [43], various enzymes involved in pathways related to glycolysis, lipids metabolism and transport have also been reported to be up-regulated, at birth, in the subcutaneous adipose tissue of the offspring. Between our three groups of rats, difference in the abundance of four key glycolytic enzymes was detected in their hypothalamus: (a) the AldoC, ubiquitous in the fetus but restricted to the brain in adult [44], involved in the production of the glyceraldehyde-3-phosphate (GAP), (b) the GAPDH, responsible for the conversion of GAP to a high-energy glycolytic compound, the 1,3-diphosphoglycerate, and the reduction of NAD+ into NADH+, (c) the alpha-enolase (Eno I), which catalyses the phosphoenolpyruvate (PEP) production and (d) the E_2PDH, which is involved in the conversion of pyruvate to acetyl-CoA (Fig. 6). Expression of AldoC was higher in RR group compared to RC pups at both stages of development, providing an ongoing source of ATP production, which is important for cytoskeletal integrity as Aldo C is associated with the actin cytoskeleton [45]. The quantity of GAPDH was significantly low in RR pups compared to RC at PND 16. At PND 12, E_2PDH, a key entry point for carbon in citric acid cycle, whose activity has been previously reported to be decreased in IUGR skeletal muscle [34] and liver [33], was significantly low in RC compared to CC pups. As the pyruvate conversion into acetyl-CoA is at the crucial branch point between two major metabolic fates (ATP production vs. substrates biosynthesis), the observed decreased E_2PDH expression is in agreement with the suggested impaired OXPHOS in IUGR followed by catch-up growth (RC). These metabolic perturbations could lead, *in fine*, to a reduction of ATP production, therefore resulting in energy shortage through alterations of fatty acid, ketone body and amino-acid biosynthesis pathways. Compared to CC, the up-regulation of the Eno I at PND 12 in RR and the down-regulation of LDH at PND 16 in RC might indicate compensatory responses to a decreased activity in the pyruvate-acetyl-coA pathway to provide sufficient pyruvate and ATP. The 19% difference in the carbohydrates contents used to balance the energy rate in both diets (8% and 20% of proteins) given to lactating mothers seems to be insufficient to explain the modifications observed in different steps of glycolysis between the RR and CC/RC groups in this study. We can, however, suggest that this supplementary dextrose level given to the restricted mothers could have an impact on the "nutrient sensing" of the hypothalamus via the content in glucose rather than on the metabolism itself.

It is now well known that the brain, the most lipid-rich organ, acquires its neural competence during development, in parallel with a switch from mixed fuel oxidation dependence, such as ketones and lactate, to a strict dependence on glucose oxidation for energy production and carbon supply [46]. In our study, at the earlier stage, when maternal protein restriction was maintained (RR), we observed an increase in the level of three enzymes involved in ketone-body pathway: the neuronal-specific Acot 7, Acat 2 and Acot 1. Acot enzymes are highly regulated by free fatty acids and are known to be a key signal in a central nutrient-sensing coupling energy balance with glucose homeostasis, particularly in β-oxidation [47]. The fact (a) that the activity of Acot has been shown to be maximal at birth and during the suckling period, a natural ketogenesis situation in rats due to the very high lipid content of rodent milk [48], (b) that it is increased, in fetal brain, when mothers received a high-fat diet [49], which is known to lead to ketogenesis [50] and (c) that maternal starvation has already been shown to increase the expression of the lactate and ketone body transporter (MCT) in placenta as well as in fetal and perinatal brain [48,51] is in agreement with this up-regulation of Acot 1, Acot

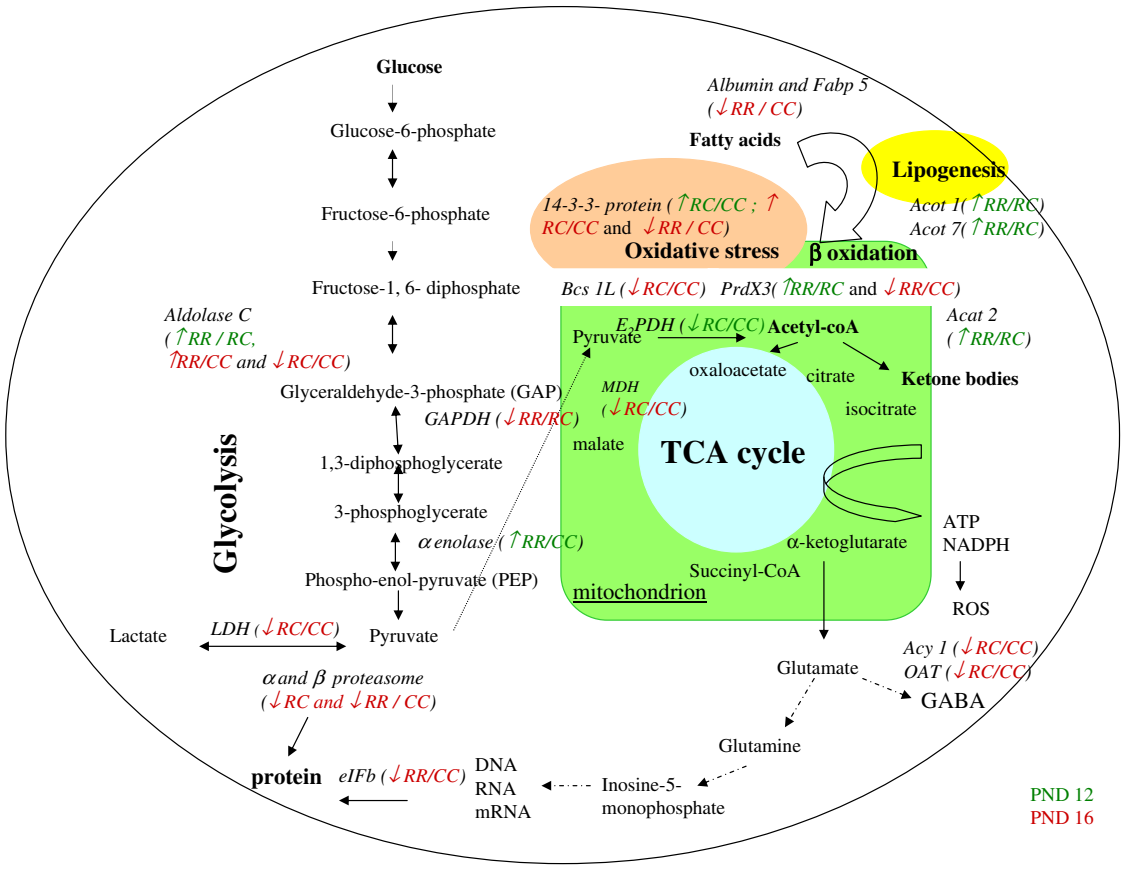

Fig. 6. Dynamic changes of proteins are schematized for RR or RC rats at PND 12 and PND 16. Proteins in green (PND12) and red (PND16) represent an elevation (↑) or diminution (↓) of expression.

7 and Acat 2 in our RR pups. Ketogenesis in astrocytes has been reported as a cytoprotective pathway [52].

At the later stage of development, the prolonged protein deprivation until weaning for RR pups, compared to CC pups, altered pathways involved in lipids binding and transport as suggested by the down-regulation of the isoform A1 of an apolipoprotein (Apo A-I) and of the serum albumin, which controls fluxes of long chain fatty acids including oleic acid and lysophosphatidic acid levels [53]. The epidermal Fabp5, previously shown to be expressed in the brain [54], to modulate acyl-coA synthesis, a fatty-acids-mediated signal transduction [55], and also to contribute to systemic glucose metabolism [56], was also down-regulated in RR pups compared to CC pups. The apolipoprotein A4 (Apo A-IV), mainly synthesized in the arcuate nucleus of the hypothalamus where it inhibits the onset of feeding, was increased in RR pups compared to RC pups at PND 12. Intestinal expression of Apo A-IV is down-regulated by leptin and up-regulated by insulin [57], and it will be informative to further study Apo A-IV regulation in the context of low leptin and insulin levels observed in our RR pups (present data). To summarize, we observed that IUGR resulted in a deregulation of key glycolytic enzymes which could result in an impaired production of NADH, ATP and acetyl-CoA production. The up-regulation, in the earlier stage, of Aldo C, Acot 1 and 7 and Acat 2 when maternal protein restriction was maintained until weaning (RR) suggests possible shunts towards alternative pathways such as ketone-body metabolism and β-oxidation, providing, respectively, the energy and carbon skeletons necessary to synthesize the precursors for lipids and cholesterol biosynthesis. These new data need to be considered in relation with the down-regulation of leptin in our RR pups [24], as the leptin signaling pathway has been recently suggested to regulate ketone bodies utilization in the hypothalamus [58].

4.3. Proteins involved in proteins or amino acids metabolism

Prolonged maternal protein starvation (RR), at the later stage of development, down-regulated proteins involved in the protein synthesis (eIF2B) and catabolism pathways (alpha and beta subunit of the proteasome type 6), compared to CC, suggesting a deregulation of brain protein turnover, both synthesis and degradation in the offspring which fit with the lower rate of protein synthesis previously reported in the IUGR rat fetal liver [59]. Rapid catch-up growth following IUGR (RC) led to the down-regulation of two important enzymes at PND 16: the ornithine aminotransferase (OAT), a key enzyme in the synaptosomal glutamate synthesis and the Arg–>Orn–>Glu–>γ-aminobutyric acid pathway [60,61], and the pyridoxal kinase (Pdxk), an enzyme known to mediate diverse reactions in the synthesis, catabolism and interconversion of amino acids and to play an important role in the neurotransmitters such as dopamine, serotonin and γ-aminobutyric acid [62]. These data could suggest an impairment in synaptic transmission associated to perinatal maternal protein restriction [63]. Oxidation rates of glutamate have been shown to be significantly blunted in isolated hepatic mitochondria from IUGR pups [33]. Finally, the aminoacylase-1A (Acy 1), an enzyme involved in protein deacetylation and suggested to play an extensive role in regulation of intermediary metabolism pathways in response to extracellular conditions [64], was down-regulated in RC compared to CC pups at PND 16.

4.4. Proteins involved in neuronal development

Several proteins involved in growth cone guidance, axonal arborization and synaptic activity have been shown to be deregulated in RC group compared to CC, such as the Arp3 of the WASP family/Arp2/3 system at PND 12 and, at the later stage, the Arp 1, the fascin and the MAPKK1. At PND 12, the prolonged maternal protein starvation (RR) up-regulated MAP2 and alpha-synuclein, both implicated in synaptic activity [65], and the chaperonin TCP-1, known to fold actin and tubulin and to facilitate synaptic activity [66]. Finally, in RR pups, at both stages of development, we observed deregulation of three members of the growth cone proteins DRPs or CRMPs (collapsin response mediator protein) whose expression was shown to be strongly regulated during development [67]: DRP2, 3 and 5. DRPs are essential signalling molecules in neuritic outgrowth, axonal guidance and synaptic plasticity [68,69] At PND 12, we have shown an increase in three isoforms of DRP2, one isoform of DRP3 and two isoforms of DRP5 in RR group compared to RC group, whereas at PND 16, another isoform of DRP5 was decreased in RC group vs. control. This is consistent with a previous published transcriptomic analysis on the same rats [20] that had shown an increase of the DpysI3 or DRP3 gene in the RR group compared to CC group at PND 12. These findings sustained our previous data [24] which reported that maternal protein restriction with or without catch-up growth could have an impact on different levels of differentiation and maturity of neurons of the hypothalamus.

To conclude, our results show that maternal protein deprivation during pregnancy only or pregnancy and lactation modulates numerous metabolic pathways resulting in alterations of hypothalamic energy supply that might, in turn, interfere with cerebral plasticity or neuronal maturation, as several of these metabolic pathways are involved in signalling pathways. More precisely, we identified several proteins which allowed, by multivariate analysis, a very good discrimination of the three groups according to their perinatal nutrition at both stages. These proteins, some of them being brain-specific, are implicated in impaired processes as (a) glycolysis (Eno 1), (b) mitochondria associated metabolism related to acetyl-CoA production, beta-oxidation (E_2PDH, Acot 1, Fabp5) or redox status (Bcs 1L, PrdX 3 and 14-3-3 protein), (c) protein metabolism (Acy1) (Fig. 6) and (d) neurogenesis and synaptogenesis (DRPs, MAP2, Snca, MAPKK1). A wide range of our data indicates alternative energy pathways such as ketone bodies production as well as lipogenesis.

Then, deciphering the alterations in cellular metabolism, redox status and cellular plasticity occurring early in life in a developing brain structure highly involved in energy metabolism may bring significant insight into the process of alterations in several functions of the brain, including nutrient sensing, regulation of feeding behaviour or stress coping, leading to the occurrence of disease at a later stage of life in individuals born with IUGR.

Supplementary data associated with this article can be found, in the online version, at doi:10.1016/j.jnutbio.2010.11.008.

References

[1] Jones RH, Ozanne SE. Fetal programming of glucose-insulin metabolism. Mol Cell Endocrinol 2009;297(1–2):4–9.
[2] Hales CN, Barker DJ. The thrifty phenotype hypothesis. Br Med Bull 2001;60:5–20.
[3] Tashima L, Nakata M, Anno K, Sugino N, Kato H. Prenatal influence of ischemia-hypoxia-induced intrauterine growth retardation on brain development and behavioral activity in rats. Biol Neonate 2001;80(1):81–7.
[4] Rolland-Cachera MF. Rate of growth in early life: a predictor of later health? Adv Exp Med Biol 2005;569:35–9.
[5] Stettler N, Stallings VA, Troxel AB, Zhao J, Schinnar R, Nelson SE, et al. Weight gain in the first week of life and overweight in adulthood: a cohort study of European American subjects fed infant formula. Circulation 2005;111(15):1897–903.
[6] Cripps RL, Archer ZA, Mercer JG, Ozanne SE. Early life programming of energy balance. Biochem Soc Trans 2007;35(Pt 5):1203–4.
[7] Ozanne SE, Hales CN. Lifespan: catch-up growth and obesity in male mice. Nature 2004;427(6973):411–2.
[8] Plagemann A, Harder T, Rake A, Melchior K, Rohde W, Dorner G. Hypothalamic nuclei are malformed in weanling offspring of low protein malnourished rat dams. J Nutr 2000;130(10):2582–9.
[9] Langley-Evans SC, Sculley DV. The association between birthweight and longevity in the rat is complex and modulated by maternal protein intake during fetal life. FEBS Lett 2006;580(17):4150–3.
[10] Fountoulakis M, Hardmaier R, Schuller E, Lubec G. Differences in protein level between neonatal and adult brain. Electrophoresis 2000;21(3):673–8.

[11] Lubec G, Krapfenbauer K, Fountoulakis M. Proteomics in brain research: potentials and limitations. Prog Neurobiol 2003;69(3):193–211.
[12] Seefeldt I, Nebrich G, Romer I, Mao L, Klose J. Evaluation of 2-DE protein patterns from pre- and postnatal stages of the mouse brain. Proteomics 2006;6(18): 4932–9.
[13] Cheon MS, Kim SH, Fountoulakis M, Lubec G. Heart type fatty acid binding protein (H-FABP) is decreased in brains of patients with Down syndrome and Alzheimer's disease. J Neural Transm Suppl 2003(67):225–34.
[14] Butterfield DA. Proteomics: a new approach to investigate oxidative stress in Alzheimer's disease brain. Brain Res 2004;1000(1–2):1–7.
[15] De Iuliis A, Grigoletto J, Recchia A, Giusti P, Arslan P. A proteomic approach in the study of an animal model of Parkinson's disease. Clin Chim Acta 2005;357(2): 202–9.
[16] Deshane J, Chaves L, Sarikonda KV, Isbell S, Wilson L, Kirk M, et al. Proteomics analysis of rat brain protein modulations by grape seed extract. J Agric Food Chem 2004;52(26):7872–83.
[17] Bouret SG, Simerly RB. Developmental programming of hypothalamic feeding circuits. Clin Genet 2006;70(4):295–301.
[18] Morgane PJ, Mokler DJ, Galler JR. Effects of prenatal protein malnutrition on the hippocampal formation. Neurosci Biobehav Rev 2002;26(4):471–83.
[19] Fanca-Berthon P, Michel C, Pagniez A, Rival M, Van Seuningen I, Darmaun D, et al. Intrauterine growth restriction alters postnatal colonic barrier maturation in rats. Pediatr Res 2009;66(1):47–52.
[20] Coupe B, Amarger V, Grit I, Benani A, Parnet P. Nutritional programming affects hypothalamic organization and early response to leptin. Endocrinology 2010;151 (2):702–13.
[21] Westermeier R, Marouga R. Protein detection methods in proteomics research. Biosci Rep 2005;25(1–2):19–32.
[22] Berth M, Moser FM, Kolbe M, Bernhardt J. The state of the art in the analysis of two-dimensional gel electrophoresis images. Appl Microbiol Biotechnol 2007;76 (6):1223–43.
[23] Coupe B, Grit I, Darmaun D, Parnet P. The timing of "catch-up growth" affects metabolism and appetite regulation in male rats born with intrauterine growth restriction. Am J Physiol Regul Integr Comp Physiol 2009;297(3):R813–24.
[24] Coupe B, Dutriez-Casteloot I, Breton C, Lefevre F, Mairesse J, Dickes-Coopman A, et al. Perinatal undernutrition modifies cell proliferation and brain-derived neurotrophic factor levels during critical time-windows for hypothalamic and hippocampal development in the male rat. J Neuroendocrinol 2009;21(1):40–8.
[25] Grigor MR, Allan JE, Carrington JM, Carne A, Geursen A, Young D, et al. Effect of dietary protein and food restriction on milk production and composition, maternal tissues and enzymes in lactating rats. J Nutr 1987;117(7):1247–58.
[26] Shen Q, Xu H, Wei LM, Chen J, Liu HM, Guo W. A comparative proteomic study of nephrogenesis in intrauterine growth restriction. Pediatr Nephrol 2010;25(6): 1063–72.
[27] Wang J, Chen L, Li D, Yin Y, Wang X, Li P, et al. Intrauterine growth restriction affects the proteomes of the small intestine, liver, and skeletal muscle in newborn pigs. J Nutr 2008;138(1):60–6.
[28] Campostrini N, Areces LB, Rappsilber J, Pietrogrande MC, Dondi F, Pastorino F, et al. Spot overlapping in two-dimensional maps: a serious problem ignored for much too long. Proteomics 2005;5(9):2385–95.
[29] Pawlyk AC, Ferber M, Shah A, Pack AI, Naidoo N. Proteomic analysis of the effects and interactions of sleep deprivation and aging in mouse cerebral cortex. J Neurochem 2007;103(6):2301–13.
[30] Becker M, Nothwang HG, Friauf E. Different protein profiles in inferior colliculus and cerebellum: a comparative proteomic study. Neuroscience 2008;154(1):233–44.
[31] Gupta P, Narang M, Banerjee BD, Basu S. Oxidative stress in term small for gestational age neonates born to undernourished mothers: a case control study. BMC Pediatr 2004;4:14.
[32] Simmons RA. Developmental origins of diabetes: the role of oxidative stress. Free Radic Biol Med 2006;40(6):917–22.
[33] Peterside IE, Selak MA, Simmons RA. Impaired oxidative phosphorylation in hepatic mitochondria in growth-retarded rats. Am J Physiol Endocrinol Metab 2003;285(6):E1258–66.
[34] Selak MA, Storey BT, Peterside I, Simmons RA. Impaired oxidative phosphorylation in skeletal muscle of intrauterine growth-retarded rats. Am J Physiol Endocrinol Metab 2003;285(1):E130–7.
[35] Gallagher EA, Newman JP, Green LR, Hanson MA. The effect of low protein diet in pregnancy on the development of brain metabolism in rat offspring. J Physiol 2005;568(Pt 2):553–8.
[36] Wallace DC. A mitochondrial paradigm of metabolic and degenerative diseases, aging, and cancer: a dawn for evolutionary medicine. Annu Rev Genet 2005;39: 359–407.
[37] Schapira AH. Mitochondrial disease. Lancet 2006;368(9529):70–82.
[38] Benani A, Troy S, Carmona MC, Fioramonti X, Lorsignol A, Leloup C, et al. Role for mitochondrial reactive oxygen species in brain lipid sensing: redox regulation of food intake. Diabetes 2007;56(1):152–60.
[39] Sandoval D, Cota D, Seeley RJ. The integrative role of CNS fuel-sensing mechanisms in energy balance and glucose regulation. Annu Rev Physiol 2008;70:513–35.
[40] Kjarland E, Keen TJ, Kleppe R. Does isoform diversity explain functional differences in the 14-3-3 protein family? Curr Pharm Biotechnol 2006;7(3): 217–23.
[41] Kobayashi-Miura M, Shioji K, Hoshino Y, Masutani H, Nakamura H, Yodoi J. Oxygen sensing and redox signaling: the role of thioredoxin in embryonic development and cardiac diseases. Am J Physiol Heart Circ Physiol 2007;292(5): H2040–50.
[42] Das KC. Thioredoxin system in premature and newborn biology. Antioxid Redox Signal 2004;6(1):177–84.
[43] Sarr O, Louveau I, Kalbe C, Metges CC, Rehfeldt C, Gondret F. Prenatal exposure to maternal low or high protein diets induces modest changes in the adipose tissue proteome of newborn piglets. J Anim Sci 2010;88(5):1626–41.
[44] Armstrong CL, Hawkes R. Pattern formation in the cerebellar cortex. Biochem Cell Biol 2000;78(5):551–62.
[45] Balaban N, Goldman R. The association of glycosomal enzymes and microtubules: a physiological phenomenon or an experimental artifact? Exp Cell Res 1990;191 (2):219–26.
[46] Pellerin L, Bergersen LH, Halestrap AP, Pierre K. Cellular and subcellular distribution of monocarboxylate transporters in cultured brain cells and in the adult brain. J Neurosci Res 2005;79(1–2):55–64.
[47] Wolfgang MJ, Lane MD. The role of hypothalamic malonyl-CoA in energy homeostasis. J Biol Chem 2006;281(49):37265–9.
[48] Nehlig A. Brain uptake and metabolism of ketone bodies in animal models. Prostaglandins Leukot Essent Fatty Acids 2004;70(3):265–75.
[49] Dierks-Ventling C, Cone AL. Acetoacetyl–coenzyme A thiolase in brain, liver, and kidney during maturation of the rat. Science 1971;172(981):380–2.
[50] Morris AA. Cerebral ketone body metabolism. J Inherit Metab Dis 2005;28(2): 109–21.
[51] Alonso de la Torre SR, Serrano MA, Medina JM. Carrier-mediated beta-D-hydroxybutyrate transport in brush-border membrane vesicles from rat placenta. Pediatr Res 1992;32(3):317–23.
[52] Guzman M, Blazquez C. Is there an astrocyte-neuron ketone body shuttle? Trends Endocrinol Metab 2001;12(4):169–73.
[53] Tabernero A, Velasco A, Granda B, Lavado EM, Medina JM. Transcytosis of albumin in astrocytes activates the sterol regulatory element-binding protein-1, which promotes the synthesis of the neurotrophic factor oleic acid. J Biol Chem 2002;277 (6):4240–6.
[54] Bennett E, Stenvers KL, Lund PK, Popko B. Cloning and characterization of a cDNA encoding a novel fatty acid binding protein from rat brain. J Neurochem 1994;63 (5):1616–24.
[55] Owada Y. Fatty acid binding protein: localization and functional significance in the brain. Tohoku J Exp Med 2008;214(3):213–20.
[56] Maeda K, Uysal KT, Makowski L, Gorgun CZ, Atsumi G, Parker RA, et al. Role of the fatty acid binding protein mal1 in obesity and insulin resistance. Diabetes 2003;52 (2):300–7.
[57] Liu M, Shen L, Doi T, Woods SC, Seeley RJ, Tso P. Neuropeptide Y and lipid increase apolipoprotein AIV gene expression in rat hypothalamus. Brain Res 2003;971(2): 232–8.
[58] Narishima R, Yamasaki M, Hasegawa S, Fukui T. Genetic obesity affects neural ketone body utilization in the rat brain. Obesity (Silver Spring) 2009;17(3): 611–5.
[59] Parimi PS, Cripe-Mamie C, Kalhan SC. Metabolic responses to protein restriction during pregnancy in rat and translation initiation factors in the mother and fetus. Pediatr Res 2004;56(3):423–31.
[60] Sadasivudu B, Swamy M. Possible occurrence of ornithine-omega-aminotransferase in GABAergic neurons. Neurochem Res 1984;9(11):1593–8.
[61] Yu H, Iyer RK, Kern RM, Rodriguez WI, Grody WW, Cederbaum SD. Expression of arginase isozymes in mouse brain. J Neurosci Res 2001;66(3):406–22.
[62] Shin JH, Weitzdoerfer R, Fountoulakis M, Lubec G. Expression of cystathionine beta-synthase, pyridoxal kinase, and ES1 protein homolog (mitochondrial precursor) in fetal Down syndrome brain. Neurochem Int 2004;45(1): 73–9.
[63] Ding Q, Vaynman S, Souda P, Whitelegge JP, Gomez-Pinilla F. Exercise affects energy metabolism and neural plasticity-related proteins in the hippocampus as revealed by proteomic analysis. Eur J Neurosci 2006;24(5):1265–76.
[64] Zhao S, Xu W, Jiang W, Yu W, Lin Y, Zhang T, et al. Regulation of cellular metabolism by protein lysine acetylation. Science 2010;327(5968):1000–4.
[65] Lavedan C. The synuclein family. Genome Res 1998;8(9):871–80.
[66] Yoo BC, Fountoulakis M, Dierssen M, Lubec G. Expression patterns of chaperone proteins in cerebral cortex of the fetus with Down syndrome: dysregulation of T-complex protein 1. J Neural Transm Suppl 2001(61):321–34.
[67] Byk T, Ozon S, Sobel A. The Ulip family phosphoproteins–common and specific properties. Eur J Biochem 1998;254(1):14–24.
[68] Hotta A, Inatome R, Yuasa-Kawada J, Qin Q, Yamamura H, Yanagi S. Critical role of collapsin response mediator protein-associated molecule CRAM for filopodia and growth cone development in neurons. Mol Biol Cell 2005;16(1):32–9.
[69] Yanagi S. Role of CRAM (CRMP5) in growth cone development and semaphorin-mediated signaling. Seikagaku 2006;78(4):291–300.